Catalysis Today 154 (2010) 293–302

Contents lists available at ScienceDirect

Catalysis Today

journal homepage: www.elsevier.com/locate/cattod

Effect of chloride on the sinterization of Au/CeO_2 catalysts

S.A.C. Carabineiro [a,*], A.M.T. Silva [a], G. Dražić [b], P.B. Tavares [c], J.L. Figueiredo [a]

[a] Laboratório de Catálise e Materiais (LCM), Laboratório Associado LSRE/LCM, Departamento de Engenharia Química, Faculdade de Engenharia, Universidade do Porto, Rua Dr. Roberto Frias s/n, 4200-465 Porto, Portugal
[b] Jozef Stefan Institute, Department of Nanostructured Materials, Jamova 39, SI-1000 Ljubljana, Slovenia
[c] CQVR Centro de Química – Vila Real, Departamento de Química, Universidade de Trás-os-Montes e Alto Douro, 5001-911 Vila Real, Portugal

ARTICLE INFO

Article history:
Available online 1 March 2010

Keywords:
Gold
Ceria
Chloride
Sinterization
Carbon monoxide
Oxidation

ABSTRACT

Gold was loaded on commercial CeO_2 and on ceria prepared by the solvothermal method (at $pK_a = 8.5$ at $T = 120$, 150 and 220 °C, and $pK_a = 26.5$ at $T = 150$ °C) by a traditional impregnation method (IMP) and by liquid-phase reductive deposition (LPRD). Activities for CO oxidation were compared and results discussed. Ceria samples prepared by IMP showed up to 1.1 wt.%. chloride present and much lower activity than those prepared by LPRD, which had no residual chloride. Full CO conversion was obtained at ~200 °C for most LPRD samples, while at that same temperature, for the IMP samples, the conversion varied from 2% (commercial ceria) to 16% (solvothermal ceria prepared at $pK_a = 8.5$ and $T = 120$ °C). Sintering of gold was quite evident in all IMP materials, possibly due to the presence of chloride. The commercial CeO_2 was the most sensitive to chloride, only achieving full CO conversion at ~700 °C, thus behaving similarly to the support. This was likely due to the large Au nanoparticle size (up to 400 nm), when compared with the solvothermal ceria (up to 200 nm). LPRD samples had lower particle sizes (ranging from 3 to 50 nm) and contain gold in the oxidic form, while IMP samples showed gold in the reduced form.

1. Introduction

Gold catalysts have recently been a "hot topic" due to their potential applications in many reactions of industrial and environmental importance [1–4]. Several variables have been considered as crucial factors influencing the chemistry, structure, and catalytic activity of gold catalysts. Among them are the method of preparation, the nature of the support, the pre-treatment and calcination procedures used and, particularly, the gold nanoparticle size [1–3].

The oxidation of carbon monoxide ($CO + ()O_2 \rightarrow CO_2$) is a commonly used test reaction for supported gold catalysts, not just due to its simplicity, but because it can have important applications, namely in CO removal from H_2 streams for fuel cells and gas sensing [1–3,5,6]. Despite the extensive research work, the mechanism and the role of the oxide support in the reaction are still under discussion.

In particular, the effect of residual chlorine on the catalytic performance in CO oxidation is not yet completely understood. The latter has been found to affect the activities of gold catalysts in different ways: facilitating the agglomeration of Au particles during heat treatment; inhibiting the reduction of gold and hindering the catalytic activity by poisoning the active sites [1,2,5–28]. Uphade et al. also reported agglomeration of Au particles after they impregnated an Au/Ti-MCM-41 catalyst with CsCl [29].

Conventional impregnation methods (incipient wetness, electrostatic adsorption, among others) generally lead to poorly active systems [7,9,12,14,24,27,30–33]. The poor performance of gold catalysts prepared by impregnation is ascribed to the presence of chloride [1–3,7,9,12,14,15,21,24,27,30,33]. According to Haruta, in the case of impregnation, a large (several tens nm in diameter) spherical Au particle is simply mixed with smaller support particles, while in the other methods, like deposition–precipitation, small hemispherical Au particles are strongly contacted with support particles at their flat planes [31]. As a reduction step of gold complex to metallic gold is required to activate gold catalysts prepared by impregnation [9], chloride can thus be removed by reduction or calcination [9,14]. However, high-temperature calcination or reduction also causes agglomeration of Au particles [1–3,15,24]. Chloride is known to have a sintering effect during thermal treatments. This is due to the ease with which gold and chloride ions combine to form bridges, favouring the growth of the particles upon heating [34,35]. Moreover, there appears to be an interface layer of Au^{3+} in the incipient wetness (IW) catalysts, even after calcination. Low loadings of Au by IW produce a thin layer of oxidized Au, which sinters during calcination, while higher

* Corresponding author: Tel.: +351 225081582; fax: +351 225081449.
E-mail address: scarabin@fe.up.pt (S.A.C. Carabineiro).

0920-5861/$ – see front matter © Elsevier B.V. All rights reserved.
doi:10.1016/j.cattod.2009.12.017

loadings produce initially chlorided catalysts [15]. Therefore, chloride removal is a very important step in the preparation of a gold catalyst. To assure chloride removal, a washing procedure is necessary.

The poisonous effect of chloride was already shown in Au/TiO_2 [7,15,24,27], Au/Al_2O_3 [6,12,27,33], Au/ZrO_2 [27] and Au/CeO_2 catalysts [21,27,36]. According to Kung et al. [6], in the case of Au/Al_2O_3 catalyst, chloride in the amount of Cl/Au atom ratio of 0.1 would decrease the activity approximately by half. The influence of the incorporation of chloride, either by the direct impregnation with HCl solution or during the deposition of Au in catalyst preparations using chloride salts as precursors, on the surface properties of CeO_2 was studied by EPR, and the existence of CeO_2–Cl species in Au/CeO_2 sample was reported [36].

However, chloride can be displaced by other anions. Addition of magnesium citrate to the preparation solution can lead to an active catalyst, as proved by several authors [8,12,37]. Chloride ions can also be displaced by hydroxide groups with the increase of pH [22]. The presence of a basic agent will permit the substitution of chloride ions by hydroxyl groups. Preparation of an Au/Al_2O_3 precursor by incipient wetness impregnation with an aqueous solution of $HAuCl_4$ and subsequent chlorine removal by treatment with NaOH at 343 K, yielded supported Au^{3+} species with a first-shell structure similar to that of Au_2O_3 and $Au(OH)_3$ that was reduced to metallic gold in reducing, inert, and oxidizing gas flows at elevated temperatures [24].

Pitchon and co-workers strongly improved the catalytic activity of their Au catalysts prepared by direct anionic exchange (DAE) on alumina [17,20,38] and other supports, by the complete removal of chloride using an ammonia washing procedure. These catalysts were resistant to an oxidative ageing treatment at 873 K and to the presence of water. This kind of treatment is similar to that proposed by Xu et al. [14]. These authors reported a new impregnation method for supporting gold on alumina using $HAuCl_4$. In this method, the acidified gold solution is contacted with alumina to adsorb gold chloride on it. After washing off the excess gold precursor, the solid is treated with ammonia to replace chloride by adsorbed hydroxide. Catalysts prepared by this method were shown to be stable up to 873 K for 100 h. Rynkowski and co-workers also proposed a DAE treatment for Mg_4Al_2 [17] and $Ce_{1-x}Zr_xO_2$ [27] catalysts.

Bowker et al. [24] have described an alternative, called the double impregnation method (DIM), in which a double impregnation of chloroauric acid and a base (Na_2CO_3) are used to precipitate out gold hydroxide within the pores of the catalyst, followed by washing. The main reason for the enhanced activity of such incipient wetness catalysts is that the double impregnation results in the deposition of Au in the pores of the titania as $Au(OH)_3$, not as gold chloride, which is what usually forms in IW methods. As a result, Cl is not associated with Au and is removed from the catalyst by washing, leading to a more active catalyst with the gold nanoparticles not poisoned or sintered by the presence of chloride [24]. There may be several advantages of this kind of approach for preparing these catalysts, such as the likely avoidance of loss of Au in the preparation. Since all the Au is precipitated in the pores before the washing procedure, the weight loading can be accurately determined without external analysis. We used this method in a previous publication dealing with Au/ceria catalysts [39]. In that work, the ceria supports were prepared by solvothermolysis and compared with a commercial sample. As ceria is extensively employed in automotive three-way emission-control catalysts, due to its capacity to undergo a rapid change in oxidation state upon changes in the redox potential of the exhaust gases [1–3], it is a material worth to study.

In the present work, we compare the traditional impregnation method (IMP) with a liquid-phase reductive deposition method (LPRD) for Au loading which, to the best of our knowledge, has only been used by Sunagawa et al. to prepare Pt and Au catalysts on Fe_2O_3, FeOOH, ZrO_2 and TiO_2 supports [40]. In LPRD, unlike IMP, a washing procedure is carried out, in order to eliminate residual chloride. Furthermore, the gold (III) ions from the precursor are hydroxylated by reaction with NaOH. We also used solvothermally prepared ceria and a commercial CeO_2 sample (as received, and after a thermal treatment in nitrogen). These catalysts were tested in the oxidation of CO, in order to assess the effect of the presence or absence of residual chloride. An Au/Fe_2O_3 gold reference catalyst, supplied by the World Gold Council (WGC) [41], was also used for comparison purposes.

2. Experimental

Solvothermal CeO_2 was prepared according to the previous publications of our group [42], using methanol, with different synthesis conditions: $pK_a = 8.5$ at $T = 120$, 150 and 220 °C, and $pK_a = 26.5$ at $T = 150$ °C. Commercial CeO_2 (Fluka) was also used for comparison, as received and treated during 2 h at 400 °C in N_2. Au was loaded on the ceria supports using $HAuCl_4{\cdot}3H_2O$ as the gold precursor (Alfa Aesar) in order to achieve 1 wt.%. content of Au, by traditional impregnation (IMP) and by liquid-phase reductive deposition (LPRD) methods [40]. Briefly, the first procedure consists of impregnating the powder sample with a solution of $HAuCl_4$, in excess, ultrasonically dispersing it for 30 min, and then drying in the oven at ~100 °C overnight. A further step of reduction is needed, by treatment in H_2 at 350 °C for 2 h. The second method (LPRD) consists of mixing a solution of $HAuCl_4$ with a solution of NaOH (with a ratio of 1:4 in weight) with stirring at room temperature. The resulting solution was aged for 24 h, in the dark, at room temperature to complete the hydroxylation of Au^{3+} ions. Then the appropriate amount of support was added to the solution and, after ultrasonic dispersion for 30 min, the suspension was aged in the oven at ~100 °C overnight. The resulting solid was washed repeatedly with distilled water, for chloride removal and dried in the oven at ~100 °C overnight.

Catalytic activity measurements for CO oxidation were performed using a continuous-flow reactor. The catalyst sample weight was 200 mg and the feed gas (5% CO, 10% O_2 in He) was passed through the catalytic bed at a total flow rate of 50 ml min^{-1}. A gold reference catalyst (Type C–Au/Fe_2O_3) was supplied by the WGC [41] and used for comparison purposes. As this catalyst contained 5% Au (and our ceria samples had 1% Au), 40 mg mass of this reference material were used in order to have the same amount of Au present, as with the ceria materials. The composition of the outgoing gas stream was determined by gas chromatography.

For comparison purposes, selected Au/ceria samples prepared by LPRD (Au/commercial ceria and Au/solvothermal ceria prepared at $pK_a = 8.5$ and $T = 120$ °C) were also treated at 350 °C in H_2 for 2 h, as done for catalysts prepared by IMP, and tested for CO oxidation.

Temperature programmed reduction (TPR) experiments were performed in an AMI-200 (Altamira Instruments) apparatus. A JEOL 2010F analytical electron microscope, equipped with a field-emission gun was used for conventional and high-resolution transmission electron microscopy (TEM and HRTEM, respectively) investigations. *Z*-contrast images were collected using a high-angle annular dark-field (HAADF) detector, in scanning transmission mode (STEM). X-ray diffraction (XRD) analysis was carried out in a PAN'alytical X'Pert MPD equipped with a X'Celerator detector and secondary monochromator (Cu Kα $\lambda = 0.154$ nm, 50 kV, 40 mA). Rietveld refinement was used to identify the phases present and to calculate the crystallite size from the XRD diffraction patterns. X-ray photoelectron spectroscopy (XPS) analysis was performed with a VG Scientific ESCALAB 200A

spectrometer using Al Kα radiation (1486.6 eV) to determine Ce and Au oxidation states. Since Cl 2p peak superimposes with the satellite peak of Ce 4p3, an accurate quantification of the amount of chloride was not possible by this technique, therefore, also a semi-quantitative determination was carried out by energy-dispersive X-ray spectrometry (EDXS). Further details of the experimental setup and analytical techniques can be found elsewhere [39].

3. Results and discussion

As shown in Table 1, an increasing temperature of solvothermal preparation (from 120 to 220 °C, at the same pK_a) caused a slight decrease in the specific surface area (from 153 to 124 m^2/g), which agrees with the literature [43]. An increase in the pK_a (from 8.5 to 26.5) at the same temperature (150 °C) caused a moderate increase in the surface area (from 138 to 157 m^2/g). The commercial ceria support used revealed a smaller area of 20 m^2/g, also similar as reported in the literature [44]. A thermal treatment on this commercial support causes a slight decrease in the surface area (17 m^2/g), as also reported by other authors [45–48].

The values of the crystallite sizes of the solvothermal samples ranged from 4.6 to 7.5 nm, depending on the preparation conditions, as determined by XRD (Table 1). An increase in the pK_a (from 8.5 to 26.5, at T = 150 °C) caused a decrease in the crystallite size from 5.7 to 4.6 nm (which agrees well with the observed increase in the surface area from 138 to 157 m^2/g). With increasing temperature of synthesis (from 120 to 220 °C, at pK_a = 8.5), the particle size increased (which agrees well with the decrease in the surface area from 153 to 124 m^2/g). In general, the values obtained are comparable to those reported in the literature [46,49–52]. When compared with the solvothermal samples, the commercial support used had XRD peaks significantly narrower and with higher intensities, characteristic of larger crystallite sizes (~53 nm) and larger degree of crystallinity. This can also be seen in the spectra with Au, shown below. The crystallite size of the commercial treated sample is not much different from the untreated sample (~54 nm). These values are comparable to the 46 nm reported for a commercial CeO_2 from Daiichi [53]. In all cases, cerianite CeO_2, with face-centered cubic (*Fm-3m*) fluorite structure, was the only phase detected by XRD [ref. JCPDS 03-065-5923]. The same fluorite structure was also reported in the literature [44–46,54–58].

The solvothermal samples consisted of ultrafine agglomerated crystallites, mostly in the form of cubes, with a body diagonal of ~3–8 nm, which correlates very well with XRD and BET results. These nanoparticles of ceria have different orientations and in some cases rounded edges are observed, as can be seen in the example of Fig. 1a, for a solvothermal sample prepared at pK_a = 8.5 and T = 120 °C.

XPS was also used to characterise the commercial ceria and a solvothermal sample (prepared at pK_a = 8.5 and T = 120 °C). The two spectra were quite similar, and so only the latter is shown (Fig. 1b). The theoretical basis for all the components of ceria has been reported in the literature [59–63]. The complex spectra can be resolved by deconvolution into eight components. The assignment of each component peak is defined in Fig. 1b, where v, v', v'', v''' represent the Ce $3d_{5/2}$ contributions and u, u', u'', u''' represent the Ce $3d_{3/2}$ contributions. For $3d_{5/2}$ of Ce(4+), a mixing

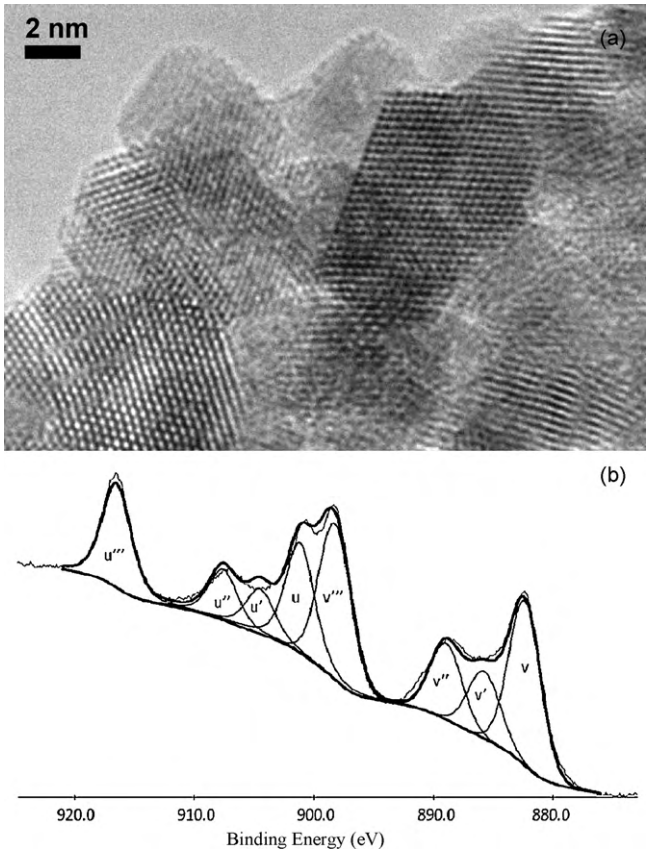

Fig. 1. HRTEM image (a) and Ce 3d XPS spectrum with peak deconvolution (b) of CeO_2 sample prepared at pK_a = 8.5 and T = 120 °C.

of the Ce $3d^9 4f^2 L^{n-2}$ and Ce $3d^9 4f^1 L^{n-1}$ states produces the peaks labeled v and v'', and the Ce $3d^9 4f^1 L^n$ final state forms the peak v'''. For $3d_{5/2}$ of Ce(3+), the Ce $3d^9 4f^2 L^{n-}$ and Ce $3d^9 4f^1 L^n$ states correspond to peaks v and v'. For Ce $3d_{3/2}$ level with the u structure, the same assignment can be carried out. A relationship between the area of CeO_2 in the Ce 3d spectra and the % of u''' peak (at ca. 917 eV, which arises from a transition of the 4f″ final state from the 4f″ initial state, and is characteristic of CeO_2, since it is absent in pure Ce_2O_3) was established by Shyu et al. [60], from which a semi-quantitative estimation of the relative amount of cerium present as Ce(IV) was made. The obtained values varied between 90% (for the solvothermal sample prepared at pK_a = 8.5 and T = 120 °C) and 98% (for commercial sample).

Fig. 2 shows the CO oxidation results obtained with all ceria samples, with and without Au, and the Au/Fe_2O_3 WGC as the reference catalyst. The solvothermally prepared ceria samples are, in general, more active than the commercial sample, as received or treated at 400 °C, with N_2, for 2 h (Fig. 2a). The most active CeO_2 solvothermal material is prepared at pK_a = 8.5 and T = 120 °C. Increasing the temperature and/or the pK_a produces less active samples. This was related with the oxygen surface content, as shown in an earlier publication [39]. In fact, it is generally accepted that CO oxidation under stationary conditions occurs over pure ceria by a Mars–van Krevelen type mechanism, where reaction

Table 1
BET surface areas (m^2/g) of ceria samples obtained by the adsorption of N_2 at 77 K, and crystallite sizes obtained by XRD (adapted from [39]).

CeO_2 samples	Commercial		Solvothermal			
	As received	Thermally treated	pK_a = 8.5, T = 120 °C	pK_a = 8.5, T = 150 °C	pK_a = 26.5 T = 150 °C	pK_a = 8.5, T = 220 °C
BET surface area (m^2/g)	20	17	153	138	157	124
Crystallite size (nm)	54	53	4.8	5.7	4.6	7.5

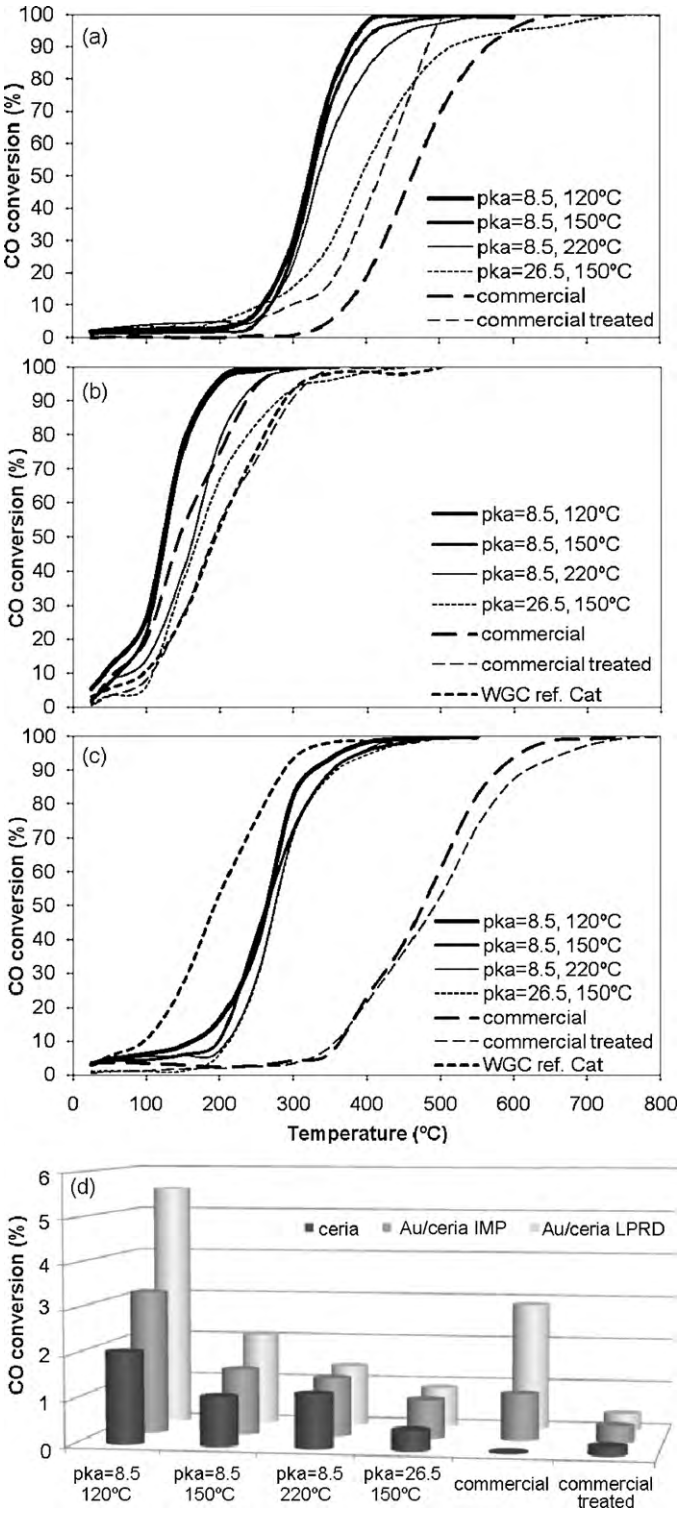

Fig. 2. CO conversion (%) versus temperature for the ceria supports (a) and Au/ceria samples prepared by LPRD (b) and IMP (c) methods. Figures (b) and (c) include the Au/Fe_2O_3 WGC reference catalyst results for comparison. CO conversion (%) at room temperature for the ceria supports and Au/ceria samples prepared by IMP and LPRD (d).

involves alternate reduction and oxidation of the ceria surface with the formation of surface oxygen vacancies (as the key step) and their successive replenishment by gas-phase oxygen, the formation and desorption of CO_2 completing the cycle [64,65].

It was shown that, for the solvothermal samples, calcination at 400 °C produces CO conversion results similar to those obtained with uncalcined materials, therefore the experiments reported in this paper were carried out with the uncalcined supports.

Loading the samples with Au (Fig. 2b and c), in general, causes CO total conversion to occur at lower temperatures, as expected, especially in the case of the solvothermal samples. Carrettin et al. reported that the addition of gold to mesoporous CeO_2 increased their activity of CO oxidation by two orders of magnitude [58]. At room temperature, the addition of Au to the solvothermal samples by either LPRD or IMP increases the CO conversion up to ~3 times, when compared to the unloaded ceria samples, as can be seen in Fig. 2d. With the commercial sample, also at room temperature, the increase is ~35 times for the IMP method (more than one order of magnitude) and ~100 times for the LPRD method (two orders of magnitude). However, Carrettin et al.'s results were obtained at 10 °C, with 0.2% of CO [58], while we used 5% of this gas.

For gold on an oxide support, it is widely accepted that a mechanism different from the Mars–van Krevelen (explained above) occurs, that is, a CO molecule is chemisorbed on a gold atom, while a hydroxyl ion moves from the support to a gold ion, creating an anion vacancy. They react to form a carboxylate group, and an oxygen molecule occupies the anion vacancy as O_2^-. This oxidizes the carboxylate group by extracting a hydrogen atom, forming carbon dioxide, and the resulting hydroperoxide ion HO_2^- then oxidizes a further carboxylate species forming another carbon dioxide and restoring two hydroxide ions to the support surface, completing the catalytic cycle. This mechanism was proposed in 2000 by Bond and Thompson [5], and has been substantiated by subsequent results of several authors [66].

With the solvothermal samples prepared at $pK_a = 8.5$, $T = 120$ and 150 °C, with Au loaded by LPRD, the CO conversion is practically total (above 95%) when the reaction temperature reaches ~200 °C (Fig. 2b) while, at that same temperature, the conversion was 53% for the WGC reference catalyst, and varied from 2% (commercial ceria) to 16% (solvothermal ceria prepared at $pK_a = 8.5$ and $T = 120$ °C) for the IMP samples (Fig. 2c). With the unloaded samples (Fig. 2a) there is practically no conversion below 200 °C (~5% maximum), full conversion being only achieved at 400–700 °C. Ceria prepared at $pK_a = 8.5$, $T = 120$ and 150 °C, with Au loaded by LPRD, are thus the most active samples in this study (Fig. 2b).

In contrast, the commercial ceria is one of the less active samples studied (along with the solvothermally prepared at $pK_a = 26.5$ and $T = 150$ °C), either pure (Fig. 2a) or loaded with Au by IMP (Fig. 2c). It can be seen that Au/commercial ceria has a better behaviour when gold is loaded by LPRD (Fig. 2b), but when the IMP method is used (Fig. 2c), above 450 °C, it becomes worse than the support itself, becoming the less active sample obtained in this study. As expected, all catalysts prepared by IMP showed a catalytic activity inferior to the reference catalyst (Fig. 2c).

For comparison purposes, Au/(commercial ceria) and Au/(solvothermal ceria synthesised at $pK_a = 8.5$ and $T = 120$ °C), prepared by LPRD, were also reduced at 350 °C in H_2 for 2 h and tested for CO oxidation (not shown). It was observed that this treatment slightly changed the catalytic behaviour of the LPRD samples, since CO conversion values were inferior to those obtained with the untreated materials. This was most likely related with the Au oxidation state, as particle size remained the same, as will be discussed below. On the other hand, not performing the reduction step in H_2 for the IMP samples yielded materials with catalytic activity similar to the ceria supports, thus showing that the presence of Au in that state did not improve the catalyst.

The samples prepared by LPRD (reduced in H_2 or not), although significantly more active than those prepared by IMP, were not as active as those prepared by the DIM method studied in the earlier paper, using the same solvothermal supports [39].

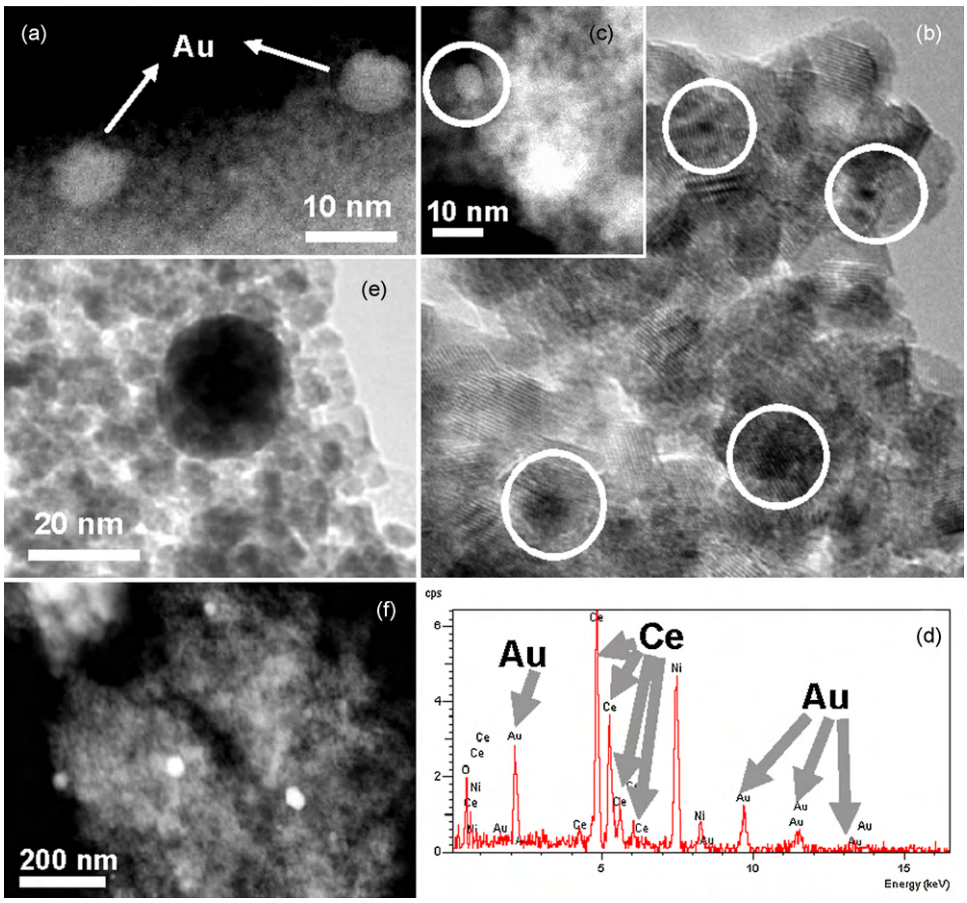

Fig. 3. Solvothermal samples with Au loaded by LPRD: HAADF image of CeO_2 sample prepared at pK_a = 8.5 and T = 120 °C (a). TEM (b) and HAADF (c) images of ceria prepared at pK_a = 8.5 and T = 150 °C, and respective EDXS spectra from a gold nanoparticle (d). TEM (e) and HAADF (f) images of CeO_2 prepared at pK_a = 8.5 and T = 220 °C.

Fig. 3 shows the HAADF (Fig. 3a and c) and HRTEM (Fig. 3b) images of the solvothermal ceria prepared at pK_a = 8.5, T = 120 and 150 °C, respectively, with Au loaded by LPRD. The presence of gold was confirmed by EDXS as displayed in Fig. 3d. These samples showed the smallest particle sizes obtained in this study (3–12 nm), which explains why they were also the most active for CO oxidation (Fig. 2b). Au particles are not agglomerated and are well dispersed on the CeO_2 support.

Fig. 3 also shows the HRTEM (Fig. 3e) and HAADF (Fig. 3f) images of the solvothermal ceria prepared at pK_a = 8.5 and T = 220 °C, with Au loaded by LPRD. This sample was not as active as the solvothermal samples prepared at lower temperature (Fig. 2b), which can be explained by its larger particle size (20–50 nm).

The commercial ceria sample (with Au loaded by the same method) had similar Au particle sizes (20–50 nm) as can be seen in Fig. 4, which agrees with their similar results also for CO oxidation (Fig. 2b). It is interesting, however, to see that the Au particles are larger than the ceria crystallites (~3–8 nm) of the solvothermal samples (Fig. 3), which is rather unusual, as traditionally it is the support that has the largest crystallite size, as it happens with the commercial sample (~54 nm), seen in Fig. 4. Some brighter pores can be seen in commercial ceria (Fig. 4f and g), which most likely are related with the preparation method.

Although the particle size of the LPRD Au/solvothermal samples is, in most cases, above the "ideal" range (below 5 nm) reported in the literature [1,3], these samples still show a catalytic behaviour slightly better than the reference catalyst, with the exception of the sample prepared at higher pK_a, that was very similar (Fig. 2b).

Fig. 5 shows TEM (Fig. 5a) and HAADF (Fig. 5b) images of the solvothermal sample prepared at pK_a = 8.5 and T = 120 °C, with Au loaded by IMP. Compared with Fig. 3a (the same sample with Au loaded by LPRD), it can be seen that the particle size of gold is much larger when using the IMP method (20–60 nm). Again, the interesting phenomenon of the larger metal particles on the smaller support crystallites is seen. The presence of chloride was confirmed by EDXS (Fig. 5c).

Fig. 5 also shows TEM (Fig. 5d) and HAADF (Fig. 5e) images also of a solvothermal sample, but prepared at 220 °C, with Au also loaded by IMP. The particle size is larger (20–150 nm) than that of the sample prepared at 120 °C with Au loaded by IMP (Fig. 5a and b) and even larger than found for the same sample with Au loaded by LPRD (Fig. 3e and f). This explains its worse performance in CO oxidation (Fig. 2c). The presence of chloride was also confirmed by EDXS (spectra not shown as it was similar to Fig. 5c).

Therefore, it was shown that increasing the pK_a and/or the temperature of preparation results in less active samples (Fig. 2), either with gold loaded or as simple supports. In addition, increasing preparation temperatures and/or pK_a causes an increase in the Au particle size deposited on these supports.

Finally, Fig. 6 shows TEM (Fig. 6a) and HAADF (Fig. 6b and c) images of the commercial ceria sample, with Au loaded by IMP, which was the less active sample found in this study. This is most likely related with the largest size of Au particles found in this study (60–400 nm). Since IMP samples have a reduction step at 350 °C in H_2, the sintering phenomenon, most likely related with chloride (its presence was confirmed by EDXS as shown in Fig. 6d), can be the responsible for the large particle sizes. In fact, from Tammann

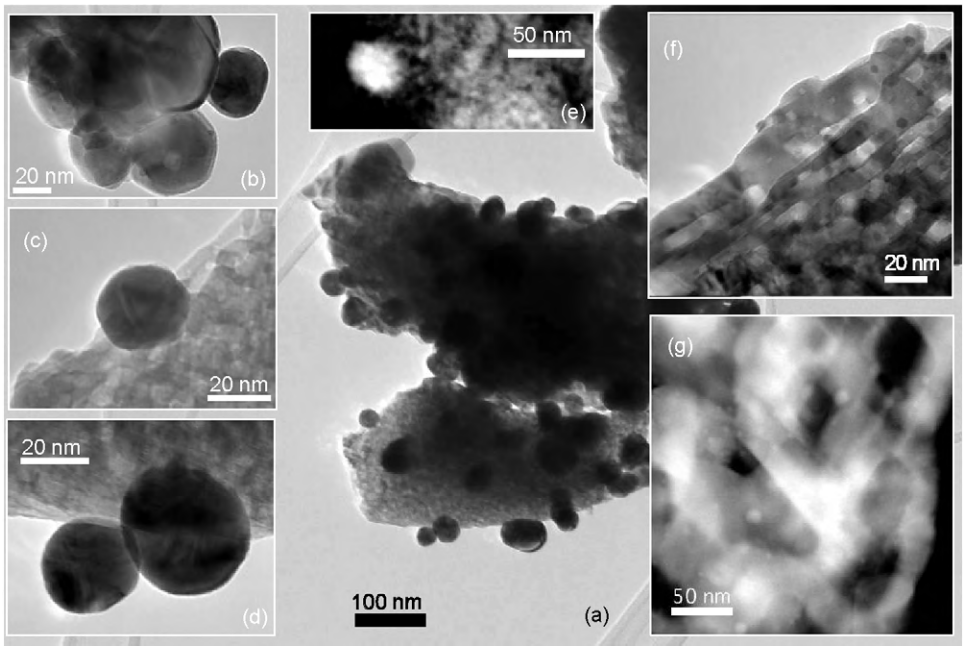

Fig. 4. TEM image of the commercial CeO_2 sample with Au loaded by LPRD (a) showing some details of the Au nanoparticles (b,c,d) and HAADF image showing an Au nanoparticle as a bright dot (e). TEM (f) and HAADF (g) images of the ceria channels with Au.

temperature considerations, gold would be expected to sinter at around 400 °C (half of the melting point of metallic gold in K). Small Au nanoparticles might well sinter at much lower temperatures than this, as their melting temperature would be expected to decrease with decreasing particle size [1,67]. Arena et al. observed the agglomeration of Au particles during the calcination step in the presence of residual chlorine, however chlorine removal during the washing treatment prevented sintering and led to the increase in activity of the studied systems [21]. In fact, the reduction treatment in H_2 for 2 h at 350 °C carried out on the chloride-free LPRD samples (commercial and solvothermal prepared at $pK_a = 8.5$ and $T = 120$ °C) which caused a slight decrease in the catalytic behaviour for CO oxidation was not due to sintering, since it was observed that the Au nanoparticle size remained similar after this treatment (not shown). This suggests that indeed it is the presence of chloride that leads to the increase in Au particle size. The decrease in the catalytic activity for CO oxidation can be due to the change in the oxidation state as it will be seen below.

Interestingly, among the IMP materials, the solvothermal samples seem to be more resistant to the sintering phenomenon,

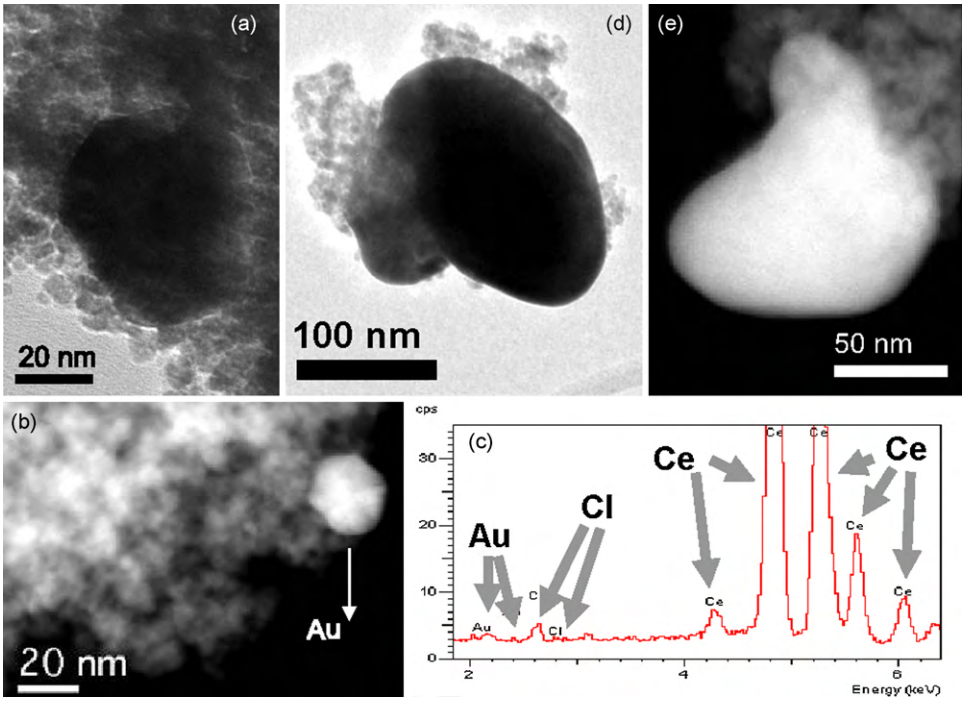

Fig. 5. Solvothermal samples with Au loaded by IMP: TEM (a) and HAADF (b) images of CeO_2 sample prepared at $pK_a = 8.5$ and $T = 120$ °C, and respective EDXS spectrum collected from average grains (c). TEM (d) and HAADF (e) images of ceria prepared at $pK_a = 8.5$ and $T = 220$ °C.

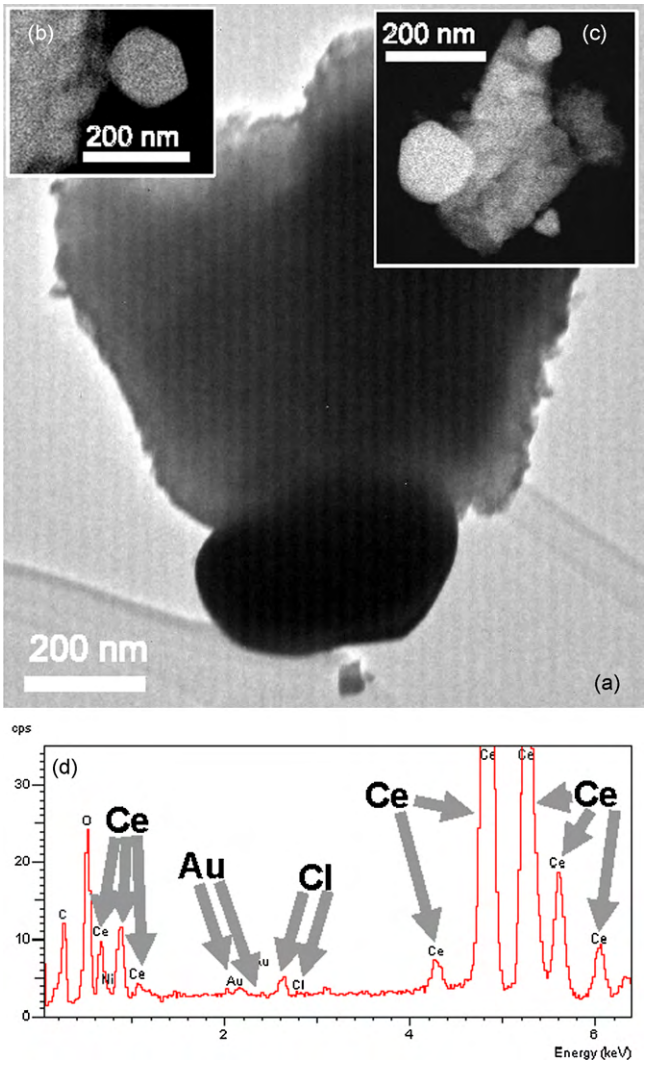

Fig. 6. TEM (a) and HAADF (b,c) images with the Au nanoparticles as bright dots of the commercial CeO_2 sample with Au loaded by IMP, and respective EDXS spectrum collected from an average of CeO_2 grains (d).

since they show smaller Au nanoparticle sizes (Fig. 5). It was shown that they possess higher amount of surface oxygen [39], so maybe this can account for their improved resistance to Cl.

An accurate quantification of the amount of chloride was not possible to obtain by XPS since the Cl 2p peak superimposes with the satellite peak of Ce 4p3, therefore, a semi-quantitative determination was carried out by EDXS. The results obtained showed that chloride was not present on the LPRD samples (Fig. 3d), but was present in the IMP ones (Fig. 5c and 6d). This technique showed that practically all chlorine present in samples was concentrated in the small (up to 20 nm) CeO_2 grains. Larger grains (up to 100 nm) contained very little amount of Cl (maximum 0.1 wt.%). The analysis was performed in the middle and on the edges of the larger grains and no difference in the Cl concentration was found (small grains were too small to perform such an analysis and often overlapped each other). It was also found that gold particles did not contain chlorine on themselves. The amount of chloride was higher in the Au/commercial ceria (up to 1.1 wt.%) than in the Au/solvothermal material (up to 0.7 wt.%). The values are similar before and after reduction in H_2, and also after the reaction of CO oxidation. For the commercial sample, a particularly interesting chloride distribution was found, since no Cl was found on a specific Au particle, but 0.6–1.1 wt.% Cl was detected on the support near to the gold particle. The location of chloride near the gold particle but not on the gold itself suggests the possibility of the formation of Au–Cl bridges, described in the literature [34,35], and needs further investigation. For the solvothermal material, no correlation was found between the Cl concentration and the Au position (although also no Cl was detected on the gold particles themselves).

Semi-quantitative EDXS results showed that the amount of Au present was around 0.8 wt.%, while XPS gave more accurate values, similar to 1%, which was the intended load in the preparation methods.

Only some traces of gold were detected by XRD in the ceria samples, as shown in Fig. 7, both for the solvothermal (a) and commercial (b) samples. The Au *Fm-3m* cubic form was identified, however it was not possible to determine accurately its particle size most likely since the loading was too low for an efficient analysis of the peaks. Not much change was found in the particle size of CeO_2 crystallite sizes upon loading with Au. As seen with the supports, the commercial ceria with Au, also had XRD peaks significantly narrower and with higher intensities, characteristic of larger crystallite sizes (~53 nm) and larger degree of crystallinity, when compared with the solvothermal ceria. The characteristic Au(1 1 1) peak is better observed in the IMP samples (inset of Fig. 7b) than in LPRD samples (inset of Fig. 7a), of course due to the larger particle size of the IMP samples referred above.

Fig. 8 shows SAED images of commercial ceria sample with Au loaded by IMP (a) and LPRD (b) and the solvothermally prepared sample at $pK_a = 8.5$ and $T = 120\ ^\circ C$ with Au loaded by IMP (c) and LPRD (d). For all samples analysed (Au/ceria), the diffracted spots correspond to the CeO_2 phase, however different crystallite sizes were present that agreed well with those determined by XRD. Gold was detected by SAED as isolated diffraction spots only in the IMP samples (Fig. 8a and c), which were the ones that showed larger Au particle size, as seen above.

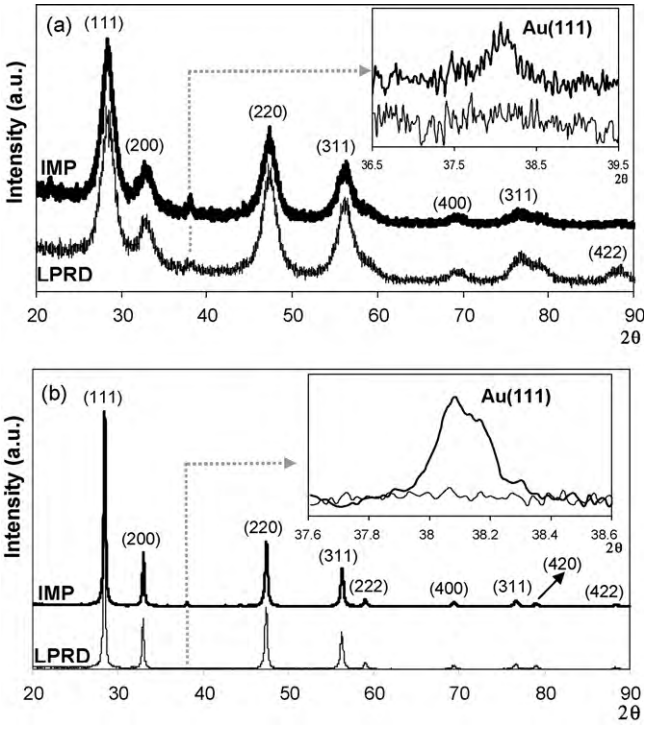

Fig. 7. XRD spectra of the CeO_2 sample prepared at $pK_a = 8.5$ and $T = 120\ ^\circ C$ (a) and the commercial sample (b) with 1% Au loaded by IMP (top, thicker lines) and LPRD (bottom, thinner lines), with ceria crystal phases identified. Insets: detail of the Au(111) peak.

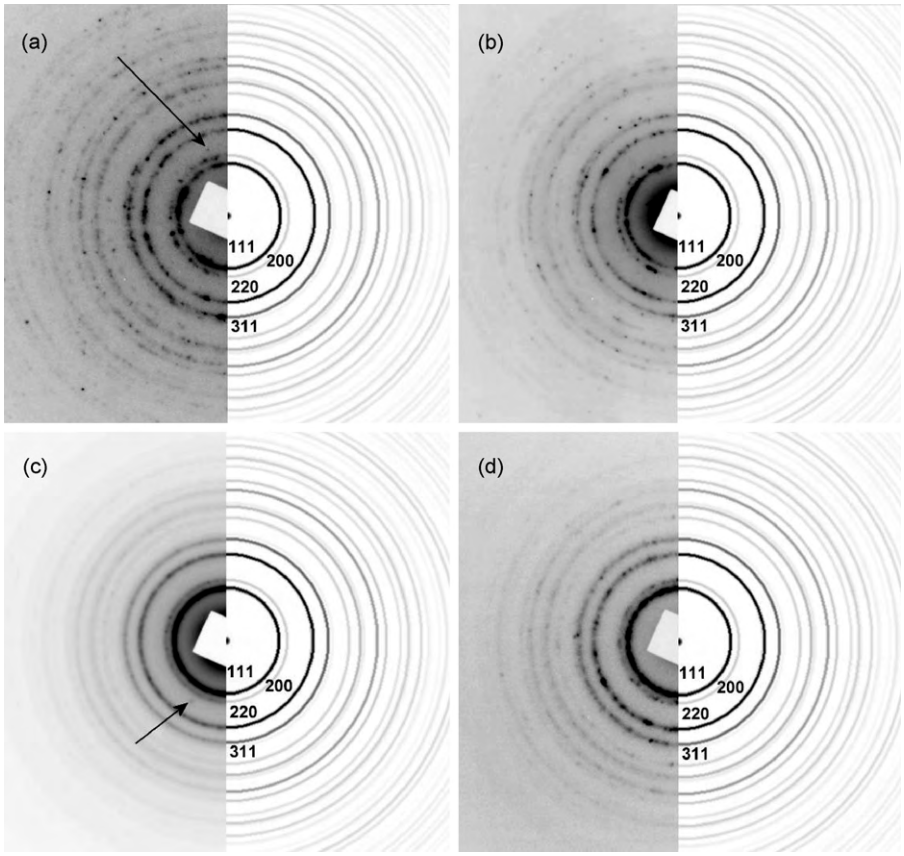

Fig. 8. SAED images of the commercial ceria sample with Au loaded by IMP (a) and LPRD (b) and the solvothermal prepared sample at pK_a = 8.5 and T = 120 °C with Au loaded by IMP (c) and LPRD (d). Arrows indicate the isolated diffraction spots attributed to Au. The right parts of the images are simulated SAED powder diffraction patterns for cubic CeO_2 with particle size of 5 nm.

TPR results are shown in Fig. 9 and demonstrate the influence of gold on ceria reducibility for the commercial sample, with and without Au. As expected from the literature [45,46,56,68–71], two peaks are seen in the TPR spectra of the pure ceria samples. The high-temperature peak (∼850° C) corresponds to the reduction of bulk oxygen and the formation of lower oxides of cerium. The first peak (∼500–600 °C) is assigned to lower temperature ceria surface shell reduction (or reduction of surface oxygen species). This peak is one order of magnitude larger for the solvothermal samples than for the commercial ceria, as previously reported, and there is a decrease in the intensity with increasing temperature and increasing pK_a, which might be related with its lower activity for CO oxidation [39]. According to the literature, the size of this first peak appears to be dependent on the method of preparation and on the amount of surface oxygen anions attached to surface Ce^{4+} ions [70]. Therefore, it can be concluded that the amount of surface oxygen is larger in the solvothermal samples than in the commercial one [39].

According to the literature, the surface shell reduction is facilitated when a metal promoter is loaded, but usually there is not much effect on the bulk oxygen of ceria [45,46,56,68–70,72]. This was also the case in the present work, although it is not so easy to tell since there is a shift to high-temperatures of the corresponding peak when Au is loaded by IMP, and the TPR experiment held until 1100 °C did not record the whole peak. In the particular case of Au, the first peak is significantly shifted to lower temperatures (∼100 °C, according to the literature, but depending on amount of Au present [44–46,56,68,69]), as it can be also observed in the spectrum of the commercial sample with Au loaded by LPRD (Fig. 9). This shift is not so evident with the IMP method, showing that the gold present is not as active as in the LPRD sample, which is in agreement with the CO oxidation results (Fig. 2). A lower reduction temperature implies that the presence of Au helps to weaken the surface oxygen on CeO_2, thereby improving the reducibility of the catalyst. This facilitates oxygen transfer across the solid–gas interface during the reaction [46,68]. Such enhanced reduction behaviour has also been observed in the case of other noble metals supported on ceria [70,71].

One single peak, at lower temperatures, is visible in the spectrum of the commercial samples loaded with Au (Fig. 9), and its area is exactly the same as the area of the corresponding peak of the Au-free sample, indicating that most gold is in metallic state, as stated by other authors [46]. In contrast, two low temperature peaks are found in the solvothermal samples with Au loaded by LPRD (not shown). The first peak can be attributed to oxygen

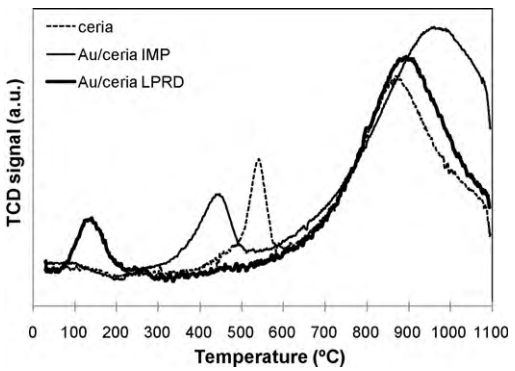

Fig. 9. H_2–TPR profiles of the pure commercial ceria sample, and with Au loaded by IMP and LPRD.

adsorbed on the surface of metallic gold and the second one to the reduction of non-metallic Au [46]. Neri et al. [73] reported two separated peaks (125 and 175 °C) for Au/Fe_2O_3 without calcination. However, after oxidation at 300 °C, only one peak (165 °C) was observed. These authors attributed the first peak to the reduction of Au oxide or hydroxide, which decomposes with calcination above 300 °C, as stated by Haruta et al. [74,75]. Solvothermal samples with Au loaded by IMP also show only one peak at low temperature (not shown), just like the commercial ceria sample (Fig. 9), which is not surprising since samples with Au loaded by this method are treated in H_2 at 350 °C before use. This peak is also shifted to lower temperatures, although this is not so evident as with the LPRD method (similarly to what was found for the commercial sample). Since the profiles of the solvothermal samples with Au loaded by LPRD showed similar results, that is, more than one peak in the lower temperature region, the contribution from oxidic gold reduction is evident.

Fig. 10 shows Au 4f XPS results for commercial (a and b) and solvothermal ceria prepared at $pK_a = 8.5$ and $T = 120$ °C (c and d), with Au loaded by IMP (a and c) and LPRD (b and d). It can be observed that samples prepared by IMP, both commercial and solvothermal ceria, have Au in the reduced form (Au^0), as expected,

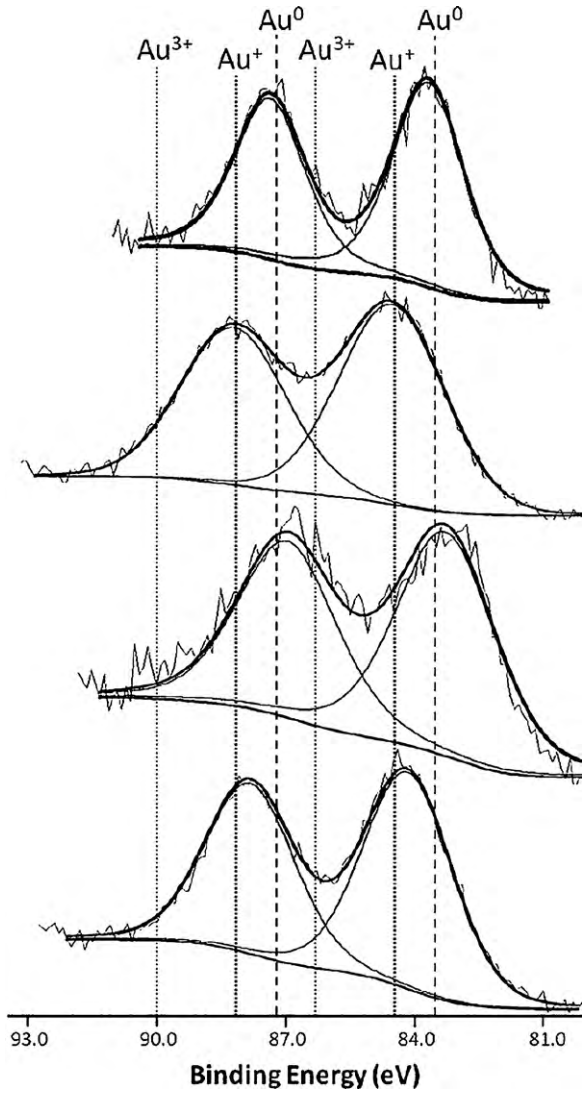

Fig. 10. Au 4f XPS spectra with peak deconvolution of Au/(commercial ceria) prepared by IMP (a) and LPRD (b), and of Au/(solvothermal ceria prepared at $pK_a = 8.5$ and $T = 120$ °C) prepared by IMP (c) and LPRD (d).

since this technique has a reduction step in H_2. Samples prepared by LPRD have Au in the oxidic state (Au^+). These findings are in agreement with the TPR results above. In fact, it is claimed that the effect of the oxidation state of gold on CO oxidation is very important, and in fact there is a strong controversy about this subject, some authors suggesting that part of the gold is non-metallic, others reporting that oxidized or partially oxidized gold species are the most active sites, while many others suggest that metallic gold is the active species [1,2].

Since non-reduced LPRD samples (gold in the Au^+ state) are more active than reduced LPRD samples (gold in the Au^0 state), and both materials have similar Au nanoparticle sizes, oxidic gold seems to plays a role in the catalytic process. In addition, the smaller particle size of gold on LPRD catalysts also accounts for the better results obtained for CO oxidation, as shown by comparing the catalytic performances of both the reduced IMP and reduced LPRD samples (both having gold in the Au^0 state, yet different particle sizes).

4. Conclusions

CeO_2 particles were prepared by the solvothermal method, which showed better performance than the commercial ceria for CO oxidation, possibly due to larger amounts of surface oxygen groups, as seen by TPR, since XRD showed that the same phase was present in all ceria samples. When gold was loaded on the samples using the LPRD method, full CO conversion was obtained at much lower temperatures. Samples prepared by IMP showed a large amount of chloride present (up to 1.1 wt.%), even after calcination, and their activity was much lower than those prepared by LPRD, which had no residual chloride, as shown by the CO oxidation tests and TPR experiments (since the surface shell oxygen reduction was much more facilitated for Cl-free samples). Sintering of gold was quite evident in all IMP materials, possibly due to the presence of chloride. The commercial CeO_2 was the most sensitive to chloride, only achieving full CO conversion at ~700 °C, thus behaving similarly to the support. This was likely due to the large Au nanoparticle size (up to 400 nm), when compared with the solvothermal ceria (up to 200 nm). The particle size of the solvothermal samples prepared at $pK_a = 8.5$, $T = 120$ and 150 °C was in the range of 3–12 nm, while the sample for $T = 220$ °C and the commercial ceria had particle sizes ranging from 20 to 50 nm. Although the gold particle size of these materials is, in most cases, far from the "ideal" range (below 5 nm) reported in the literature, these samples still show a catalytic behaviour equal or slightly better than the WGC reference catalyst. LPRD samples had gold in the oxidic form, as shown by TPR and XPS, but IMP samples showed it only in the reduced form.

Acknowledgments

Authors acknowledge Fundação para a Ciência e Tecnologia (FCT), Portugal, and the Ministry of Higher Education, Science and Technology, from Slovenia, for financial support from the Portugal–Slovenia Cooperation in Science and Technology (2008–2009), project "Synthesis and Characterization of Nanostructured Catalytic Materials". Further support from FCT and FEDER was provided under project REEQ/1106/EQU/2005. SAC and AMTS also acknowledge FCT for financing (CIENCIA 2007 program and POCI/N010/2006 project, respectively). GD acknowledges the financial support of the Slovenian Research Agency.

References

[1] G.C. Bond, C. Louis, D.T. Thompson, in: G.J. Hutchings (Ed.), Catalysis by Gold, Imperial College Press, London, 2006, , references cited therein.

[2] S.A.C. Carabineiro, D.T. Thompson, Catalytic applications for gold nanotechnology, in: U. Heiz, U. Landman (Eds.), Nanocatalysis, Springer-Verlag, Berlin, Heidelberg, New York, 2007, pp. 377–489 (ISBN-13 978-3-540-32645-8) and references cited therein.
[3] S.A.C. Carabineiro, D.T. Thompson, Gold catalysis, in: C. Corti, R. Holliday (Eds.), Gold: Science and applications, CRC Press, Taylor and Francis Group, Boca Raton, London, New York, 2010 pp. 89–122, (ISBN-978-1-4200-6523-7) and references cited therein.
[4] C.W. Corti, R.J. Holliday, D.T. Thompson, Top. Catal. 44 (2007) 331.
[5] G.C. Bond, D.T. Thompson, Gold Bull. 33 (2000) 41.
[6] H.H. Kung, M.C. Kung, C.K. Costello, J. Catal. 216 (2003) 425.
[7] S.D. Lin, M. Bollinger, M.A. Vannice, Catal. Lett. 17 (1993) 245.
[8] G.C. Bond, D.T. Thompson, Catal. Rev. Sci. Eng. 41 (1999) 319.
[9] Y.J. Chen, C.T. Yeh, J. Catal. 200 (2001) 59.
[10] A. Wolf, F. Schuth, Appl. Catal. A 226 (2002) 1.
[11] M. Haruta, Cattech 6 (2002) 102.
[12] H.S. Oh, J.H. Yang, C.K. Costello, Y. Wang, S.R. Bare, H.H. Kung, M.C. Kung, J. Catal. 210 (2002) 375.
[13] C.K. Costello, M.C. Kung, H.S. Oh, Y. Wang, H.H. Kung, Appl. Catal. A 232 (2002) 159.
[14] Q. Xu, K.C.C. Kharas, A. Datye, Catal. Lett. 85 (2003) 229.
[15] J.M.C. Soares, P. Morrall, A. Crossley, P. Harris, M. Bowker, J. Catal. 219 (2003) 17.
[16] R. Meyer, C. Lemire, S.K. Shaikhutdinov, H.-J. Freund, Gold Bull. 37 (2004) 72.
[17] I. Dobrosz, K. Jiratova, V. Pitchon, J.M. Rynkowski, J. Mol. Catal. A 234 (2005) 187.
[18] A. Jain, X. Zhao, S. Kjergaard, S.M. Stagg-Williams, Catal. Lett. 104 (2005) 191.
[19] S. Ivanova, V. Pitchon, Y. Zimmermann, C. Petit, Appl. Catal. A 298 (2006) 57.
[20] S. Ivanova, C. Petit, V. Pitchon, Gold Bull. 39 (2006) 3.
[21] F. Arena, P. Famulari, G. Trunfio, G. Bonura, F. Frusteri, L. Spadaro, Appl. Catal. B 66 (2006) 81.
[22] H. Zhu, C. Liang, W. Yan, S.H. Overbury, S. Dai, J. Phys. Chem. B 110 (2006) 10842.
[23] M.C. Kung, R.J. Davis, H.H. Kung, J. Phys. Chem. C 111 (2007) 11767.
[24] M. Bowker, A. Nuhu, J. Soares, Catal. Today 122 (2007) 245.
[25] E. Bus, R. Prins, J.A. van Bokhoven, Phys. Chem. Chem. Phys. 9 (2007) 3312.
[26] C.G. Long, J.D. Gilbertson, G. Vijayaraghavan, K.J. Stevenson, C.J. Pursell, B.D. Chandler, J. Am. Chem. Soc. 130 (2008) 10103.
[27] A. Hugon, L. Delannoy, C. Louis, Gold Bull. 41 (2008) 127.
[28] I. Dobrosz-Gómez, I. Kocemba, J.M. Rynkowski, Appl. Catal. B 88 (2009) 83.
[29] B.S. Uphade, M. Okumura, S. Tsubota, M. Haruta, Appl. Catal. A 190 (2000) 43.
[30] M. Haruta, Catal. Today 36 (1997) 153.
[31] A.I. Kozlov, A.P. Kozlova, H. Liu, Y. Iwasawa, Appl. Catal. A 182 (1999) 9.
[32] M. Haruta, M. Daté, Appl. Catal. A 222 (2001) 427.
[33] S.J. Lee, A. Gavriilidis, J. Catal. 206 (2002) 305.
[34] M. Hargittai, A. Schulz, B. Reffy, M. Kolonits, J. Am. Chem. Soc. 123 (2001) 1449.
[35] A. Schulz, M. Hargittai, Chem. Eur. J. 7 (2001) 3657.
[36] J. Soria, J.C. Conesa, A. Martýnez-Arias, Colloid Surf. A: Phys. Eng. Aspect 158 (1999) 67.
[37] G.K. Bethke, H.H. Kung, Appl. Catal. A 194/195 (2000) 43.
[38] S. Ivanova, V. Pitchon, C. Petit, J. Mol. Catal. A 256 (2006) 278.
[39] S.A.C. Carabineiro, A.M.T. Silva, G. Dražić, P.B. Tavares, J.L. Figueiredo, Catal. Today, in press, (doi:10.1016/j.cattod.2010.01.036).
[40] Y. Sunagawa, K. Yamamoto, H. Takahashi, A. Muramatsu, Catal. Today 132 (2008) 81.
[41] See World Gold Council Catalysts website: http://www.utilisegold.com/uses_applications/catalysis/reference_catalysts/.
[42] A.M.T. Silva, B.F. Machado, H.T. Gomes, J.L. Figueiredo, G. Dražić, J.L. Faria, J. Nanopart. Res. 12 (2010) 121.
[43] E. Verdon, M. Devalette, G. Demazeau, Mater. Lett. 25 (1995) 127.
[44] U.R. Pillai, S. Deevi, Appl. Catal. A 299 (2006) 266.
[45] S.-Y. Lai, Y. Qiu, S. Wang, J. Catal. 237 (2006) 303.
[46] Q. Fu, S. Kudriavtseva, H. Saltsburg, M. Flytzani-Stephanopoulos, Chem. Eng. J. 93 (2003) 41.
[47] C.H. Kim, L.T. Thompson, J. Catal. 230 (2005) 66.
[48] A. Karpenko, R. Leppelt, V. Plzak, J. Cai, A. Chuvilin, B. Schumacher, U. Kaiser, R.J. Behm, Top. Catal. 44 (2007) 183.
[49] X. Zheng, S. Wang, X. Wang, S. Wang, X. Wang, S. Wu, Mater. Lett. 59 (2005) 2769.
[50] Z.R. Tang, J.K. Edwards, J.K. Bartley, S.H. Taylor, A.F. Carley, A.A. Herzing, G.J. Hutchings, J. Catal. 249 (2007) 208.
[51] M. Manzoli, A. Chiorino, F. Boccuzzi, Stud. Surf. Sci. Catal. 155 (2005) 405.
[52] M. Manzoli, G. Avgouropoulos, T. Tabakova, J. Papavasiliou, T. Ionnides, F. Boccuzzi, Catal. Today 138 (2008) 239.
[53] V. Aguilar-Guerrero, B.C. Gates, J. Catal. 260 (2008) 351.
[54] A.I.Y. Tok, F.Y.C. Boey, Z. Dong, X.L. Sung, J. Mater. Process. Technol. 190 (2007) 217.
[55] P.X. Huang, F. Wu, B.L. Zhu, X.P. Gao, H.Y. Zhu, T.Y. Yan, W.P. Huang, S.H. Wu, D.Y. Song, J. Phys. Chem. B 109 (2005) 19169.
[56] Q. Fu, W. Deng, H. Saltsburg, M. Flytzani-Stephanopoulos, Appl. Catal. B 56 (2005) 57.
[57] Z.-Y. Yuan, V. Idakiev, A. Vantomme, T. Tabakova, T.-Z. Ren, B.-L. Su, Catal. Today 131 (2008) 203.
[58] S. Carrettin, P. Concepción, A. Corma, J.M.L. Nieto, V.F. Puntes, Angew. Chem. Int. Ed. 43 (2004) 2538.
[59] C. Pan, D. Zhang, L. Shi, J. Fang, Eur. J. Inorg. Chem. (2008) 2429.
[60] J.Z. Shyu, K. Otto, W.L.H. Watkins, G.W. Graham, R.K. Belitz, H.S. Gandhi, J. Catal. 114 (1988) 23.
[61] C. Sun, H. Li, L. Chen, J. Phys. Chem. Solids 68 (2007) 1785.
[62] S. Tsunekawa, T. Fukuda, A. Kasuya, Surf. Sci. 457 (2000) L437.
[63] V. Matolín, I. Matolínová, L. Sedláček, K.C. Prince, T. Skála, Nanotechnology 20 (2009) 215706.
[64] E. Aneggi, J. Llorca, M. Boaro, A. Trovarelli, J. Catal. 234 (2005) 88.
[65] E. Aneggi, M. Boaro, C. de Leitenburg, G. Dolcetti, A. Trovarelli, J. Alloys Compd. 408–412 (2006) 1096.
[66] G.C. Bond, D.T. Thompson, Gold Bull. 42 (2009) 247.
[67] P. Buffat, J.P. Borel, Phys. Rev. A 13 (1976) 2287.
[68] A.M. Venezia, G. Pantaleo, A. Longo, G. Di Carlo, M. Casaletto, F.L. Liotta, G. Deganello, J. Phys. Chem. B 109 (2005) 2821.
[69] D. Andreeva, V. Idakiev, T. Tabakova, L. Ilieva, P. Falaras, A. Bourlinos, A. Travlos, Catal. Today 72 (2002) 51.
[70] B. Harrison, A.F. Diwell, C. Hallett, Platinum Met. Rev. 32 (1988) 73.
[71] G. Jacobs, E. Chenu, P.M. Patterson, L. Williams, D. Sparks, G. Thomas, B.H. Davis, Appl. Catal. A 258 (2004) 203.
[72] A. Sepulveda-Escribano, F. Coloma, F. Rodriguez-Reinoso, J. Catal. 178 (1998) 649.
[73] G. Neri, A.M. Visco, S. Galvagno, A. Donato, M. Panzalorto, Therm. Acta 329 (1999) 39.
[74] M. Haruta, N. Yamada, T. Kobayashi, S. Iijima, J. Catal. 115 (1989) 301.
[75] M. Haruta, S. Tsubota, T. Kobayashi, J. Kageyama, M.J. Genet, B. Delmon, J. Catal. 144 (1993) 175.